lolal Is an Evolutionarily New Epigenetic Regulator of *dpp* Transcription during Dorsal–Ventral Axis Formation

Janine C. Quijano,[†,1] Robert G. Wisotzkey,[2] Nancy Lan Tran,[1] Yunxian Huang,[3] Michael J. Stinchfield,[1] Theodor E. Haerry,[4] Osamu Shimmi,[3] and Stuart J. Newfeld[*,1]

[1]School of Life Sciences, Arizona State University

[2]Dept. Biological Sciences, California State University–East Bay

[3]Institute of Biotechnology, University of Helsinki, Helsinki, Finland

[4]Center for Molecular Biology and Biotechnology, Florida Atlantic University

[†]Present address: Beckman Research Institute of City of Hope, Duarte CA

[*]**Corresponding author**: E-mail: newfeld@asu.edu.

Associate editor: John True

Abstract

Secreted ligands in the Dpp/BMP family drive dorsal–ventral (D/V) axis formation in all Bilaterian species. However, maternal factors regulating Dpp/BMP transcription in this process are largely unknown. We identified the BTB domain protein *longitudinals lacking-like* (*lolal*) as a modifier of *decapentaplegic* (*dpp*) mutations. We show that Lolal is evolutionarily related to the Trithorax group of chromatin regulators and that *lolal* interacts genetically with the epigenetic factor *Trithorax-like* during Dpp D/V signaling. Maternally driven Lolal^{HA} is found in oocytes and translocates to zygotic nuclei prior to the point at which *dpp* transcription begins. *lolal* maternal and zygotic mutant embryos display significant reductions in *dpp*, pMad, and *zerknullt* expression, but they are never absent. The data suggest that *lolal* is required to maintain *dpp* transcription during D/V patterning. Phylogenetic data revealed that *lolal* is an evolutionarily new gene present only in insects and crustaceans. We conclude that Lolal is the first maternal protein identified with a role in *dpp* D/V transcriptional maintenance, that Lolal and the epigenetic protein Trithorax-like are essential for Dpp D/V signaling and that the architecture of the Dpp D/V pathway evolved in the arthropod lineage after the separation from vertebrates via the incorporation of new genes such as *lolal*.

Key words: **BTB domain, Dpp/Mad/BMP/TGF-*β*, *Drosophila*, development, new gene evolution.**

Introduction

Genetic screens for modifiers of *decapentaplegic (dpp)* mutations have identified many highly conserved signal transduction pathway components essential for *Drosophila* dorsal–ventral axis formation (e.g., the prototype Smad protein *Mad*; Sekelsky et al. 1995). Each of these factors is maternally supplied as either RNA or protein, in effect "priming" embryonic cells for a rapid response to the earliest zygotic genes. In *Drosophila melanogaster*, the maternal to zygotic transition begins with a small number of transcribed genes during nuclear cycle 8 in the syncytial embryo (Pritchard and Schubiger 1996). Zygotic transcription ramps up slowly with dorsally restricted *dpp* expression first visible during nuclear cycle 10 (Jackson and Hoffmann 1994). Two maternal proteins required for the global activation of early zygotic genes, including *dpp*, are the ubiquitous transcription factors Zelda and Stat92E (Liang et al. 2008; Tsurumi et al. 2011).

Extracellular interactions generate the highest levels of Dpp activity in dorsal-most regions. Dpp signal transduction is stimulated when the ligand binds the type I receptors Thickveins (Tkv) and Saxophone (Sax) together with the type II receptor Punt. These transmembrane kinases then phosphorylate the signal transducer Mad. Phosphorylated Mad (pMad) translocates to the nucleus where it joins its sister Smad protein Medea to regulate target genes. Maximum Dpp activity stimulates genes such as *zerknullt (zen)* that drive dorsal-most cells to become amnioserosa. Repression of *dpp* transcription in ventral-most cells by Dorsal permits the activation of Twist and propels these cells to become mesoderm. One mechanism of Dpp pathway termination is monoubiquitylation of Medea by Nedd4. Subsequently, the pathway is reset by Medea activation via deubiquitylation by Fat Facets (Shimmi and Newfeld 2013).

Notwithstanding the reversal of D/V polarity between insect and vertebrate embryos (insect "nerve cords" develop on the ventral side) the signaling pathway dictating D/V polarity in both phyla is extraordinarily conserved. In vertebrates, a ventralizing gradient of Bone Morphogenetic Protein (BMP) employs homologous extracellular and signal transducing proteins in the same manner as the insect Dpp dorsalizing gradient (Bier and De Robertis 2015). An exception to universal conservation in the pathway was recently reported with the Medea ubiquitylase Nedd4 (an HECT class enzyme) replaced in the vertebrate lineage by the vertebrate-specific Smad4

ubiquitylase TIF1-γ/TRIM33 (a RING class enzyme; Wisotzkey et al. 2014).

Building upon a prior genetic screen, we found that *longitudinals lacking-like (lolal)*, which encodes a BR-C, Ttk and Bab (BTB) domain protein related to the Trithorax group of epigenetic markers, has a role in Dpp D/V signaling. In the absence of maternal and zygotic *lolal*, transcription of *dpp* is significantly reduced. This leads to abnormal pMad, reduced *zen* expression, and ventralization of the embryo. Phylogenetic studies revealed that *lolal* is an evolutionarily new gene present only in insects and crustaceans. Overall the data reveals three new insights: that Lolal is the first maternal protein identified with a role in *dpp* D/V transcriptional maintenance, that Lolal and the epigenetic protein Trl are essential for Dpp D/V signaling and that the architecture of the Dpp D/V pathway evolved in the arthropod lineage after the separation from vertebrates via the incorporation of new genes such as *lolal*.

Results

Lolal Is a Dominant Maternal Enhancer of *dpp* in D/V Patterning

The deletion *Df(2R)Pcl-11B* was identified as a dominant maternal enhancer of the recessive allele dpp^{hr4} but the responsible gene was not shown (Nicholls and Gelbart 1998). We examined ten lethal P-element insertions within the deleted region for maternal enhancement of dpp^{hr4}. $P\{lacW\}^{k02512}$ an insertion in the 5′ UTR of *lolal* (CG5738; also known as *batman)* displayed strong dominant maternal enhancement (fig. 1; supplementary table S1, Supplementary Material online). We generated two new *lolal* mutations via P element excision ($lolal^{1122}$ and $lolal^{1722}$) and confirmed that these did not affect the adjacent gene *adipose* via obesity tests (Wisotzkey et al. 2003). The two excision alleles and the *lolal* insertion allele $P\{EP\}^{G9603}$ failed to complement each other or *Df(2R)Pcl-11B* (supplementary table S2, Supplementary Material online). Repeating the dominant maternal enhancement assay revealed that *Df(2R)Pcl-11B* and the *lolal* alleles phenocopied the effect of mutations in *Mad* and *Medea*. The reverse cross with maternal dpp^{hr4} had no effect (supplementary table S1, Supplementary Material online).

To extend these results, we performed dominant maternal enhancement rescue experiments with UASP transgenes of Lolal, activated Tkv, activated Sax, activated Medea, and Trithorax-like (Trl) under the control of the maternal driver nos.Gal4. In every case, a substantive rescue was observed. Lolal and $Lolal^{HA}$ rescue of $lolal^{1122}$ enhancement generated roughly 75% of expected progeny versus 6% without Lolal. Rescue of $lolal^{1122}$ enhancement by activated Tkv, activated Medea and Trl was 100% of expected. Significant rescue in all cases was also achieved in maternal enhancement assays with the more severe allele dpp^{hr27} (fig. 2, supplementary fig. S1, and supplementary tables S2 and S3, Supplementary Material online). It appears that the presence of activated receptors or signal transducers can supplement the attenuated Dpp signal in enhanced embryos to the point at which feedback mechanisms (Wang and Ferguson 2005) are able to restore the pathway. From this perspective, the rescue data suggest that *lolal* enhancement of *dpp* occurs upstream of Dpp receptors and signal transducers.

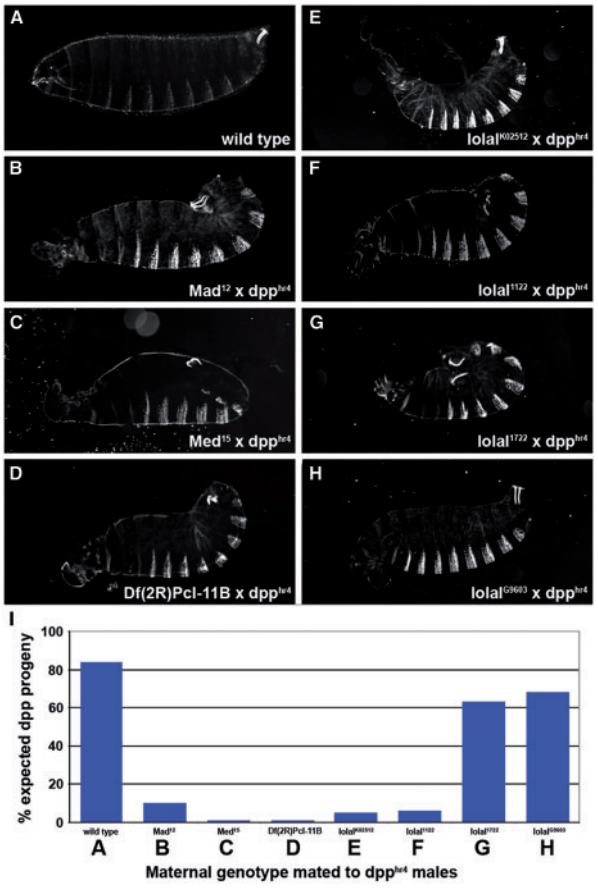

Fig. 1. *lolal* dominant maternal enhancement of *dpp*. Cuticles from the progeny of crosses between the indicated heterozygous females (except Med^{15} females were homozygous) and males heterozygous for dpp^{hr4} are shown. Anterior is to the left and dorsal up with the maternal genotype listed first. (*A*) Wild-type with the head skeleton (left), ventral denticle belts (bottom), and Filzkorper (top right) visible. (*B*) Mad^{12} progeny with a ventralized phenotype containing a curved body, dorsally extended denticles, herniated head, and defective Filzkorper. (*C*) Med^{15} progeny shows a more pronounced ventralized phenotype. (*D*) *Df(2R)Pcl-11B* progeny are similar to those of Mad^{12}. (*E*) $lolal^{KO2512}$, (*F*) $lolal^{1122}$, (*G*) $lolal^{1722}$, and (*H*) $lolal^{G9603}$ progeny are also ventralized. (*I*) Graph of progeny adult viability from the crosses shown above. Bars are connected to panels by letters and numerical data is shown in supplementary table S1, Supplementary Material online.

Consistent with the rescue data, in two *Drosophila* S2 cell assays ds-*lolal* did not prevent pMad activation or Dpp-dependent reporter gene activation. These cell-based assays indicate no role for *lolal* in Dpp signal transduction (supplementary fig. S2, Supplementary Material online). Analysis of *lolal* mutant embryos did not reveal any Dpp-dependent phenotypes and stage of lethality assays showed that *lolal* mutants die as pupae rather than as larva, like mutants for *Mad* and *Medea* (supplementary figs. S3 and S4 and supplementary tables S5 and S6, Supplementary Material online). These mutant studies suggest there is no role for *lolal* in

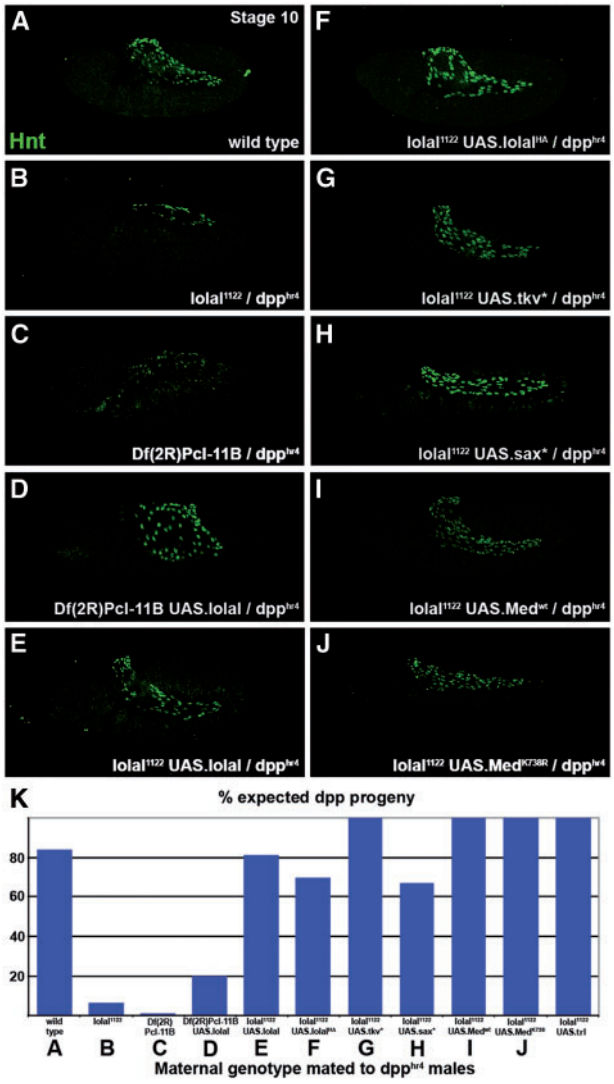

Fig. 2. Maternal expression of Lolal, Dpp pathway components or Trl rescues *lolal* dominant maternal enhancement of *dpp*. Stage 10 embryos with anterior to the left and dorsal up displaying Dpp-dependent Hindsight (green) in amnioserosa cells. The maternal genotype is listed first as a heterozygous female or a heterozygous female carrying a UASP transgene driven maternally by nos.Gal4. The paternal genotype is dpp^{hr4}. (*A*) Wild type. (*B*) Maternal $lolal^{1122}$ yields little Hindsight. (*C*) Maternal *Df(2R)Pcl-11B* yields no Hindsight. (*D*) Maternal *Df(2R)Pcl-11B* with Lolal partially rescues Hindsight. (*E*) Maternal $lolal^{1122}$ with Lolal fully rescues Hindsight. (*F*) $Lolal^{HA}$, (*G*) Tkv*, (*H*) Sax*, (*I*) Med^{wt}, and (*J*) Med^{K738R} also fully rescue Hindsight. (*K*) Graph of progeny adult viability from the crosses above. Bars are connected to panels by letters and numerical data is shown in supplementary table S3, Supplementary Material online. The bar at the far right shows complete rescue of $lolal^{1122}$ dominant maternal enhancement of dpp^{hr4} by maternal expression of Trl.

embryonic development beyond D/V patterning. Analysis of *lolal* somatic clones in larval and pupal wing disks indicated that loss of *lolal* had no effect on *dpp* transcription, pMad expression, or Dpp target gene activation (e.g., *brinker*-lacZ; supplementary fig. S5, Supplementary Material online). Collectively the S2 cell assays, zygotic mutant data, and wing disk clone results imply that *lolal* only plays a role in Dpp signaling during D/V patterning.

Maternal $Lolal^{HA}$ Translocates to the Nucleus Prior to *dpp* Transcription

lolal dominant maternal enhancement of *dpp* suggests that *lolal* RNA and protein are generated during oogenesis and deposited in unfertilized eggs as are *Mad* and *Medea*. We found *lolal* RNA in ovarioles plus *lolal* maternal RNA and protein ubiquitously distributed in unfertilized eggs (detected as translated $Lolal^{HA}$ expressed via nos.Gal4; fig. 3 and supplementary fig. S6, Supplementary Material online). This is consistent with a study reporting that *lolal* RNA is present in the embryo prior to the maternal to zygotic transition (Fisher et al. 2012). At stage 5, *lolal* zygotic RNA is ubiquitously present, a spatial distribution indicating that *lolal* is not a target of Dpp signaling.

We then examined $Lolal^{HA}$ expression during the maternal to zygotic transition (fig. 3 and supplementary fig. S6, Supplementary Material online). $Lolal^{HA}$ rescues *lolal* enhancement of dpp^{hr4} providing confidence that $Lolal^{HA}$ mimics the activity of endogenous Lolal. In these assays, we employed Bonus as a marker for developmental timing. Bonus migrates into nuclei at the maternal to zygotic transition (Wisotzkey et al. 2014). If Lolal migrates into nuclei coincidently with Bonus, then it will be in place to modulate *dpp* transcription. At nuclear cycle 8 prior to the initiation of zygotic transcription (Pritchard and Schubiger 1996), $Lolal^{HA}$, and Bonus are ubiquitous in the cytoplasm and absent from nuclei. At cycle 9, the initiation of the transition, $Lolal^{HA}$, and Bonus are present in both the cytoplasm and nuclei indicating that at least a fraction of each protein has translocated into nuclei. This is prior to the initiation of *dpp* transcription in cycle 10 (Jackson and Hoffmann 1994). By cycle 12, $Lolal^{HA}$ and Bonus are further concentrated in nuclei and nuclear localization is complete by cycle 14. The RNA and protein expression data suggested the hypothesis that *lolal* dominant maternal enhancement of *dpp* mutations is due to Lolal regulation of *dpp* transcription, an unprecedented result for a dominant maternal enhancement screen.

Lolal Is Required to Maintain Normal Levels of *dpp* Transcription

To test the hypothesis that *lolal* is necessary for *dpp* transcription, we generated $lolal^{1122}$ maternally mutant eggs via germline clone bearing females (*lolal GLC*). These females were mated to heterozygous $lolal^{1722}$ males. The enhancement and expression data suggests that expression of *dpp* will be reduced during D/V patterning in the half of progeny that are *lolal* GLC homozygous mutant embryos. These have neither a maternal nor a paternal source of functional *lolal* and will display D/V defects. The other half, the *lolal* GLC heterozygous mutant embryos, will have a paternal copy of *lolal*, and the zygotic mutant data suggests that they will appear wild type. Analysis of GLC cuticles (supplementary table S7,

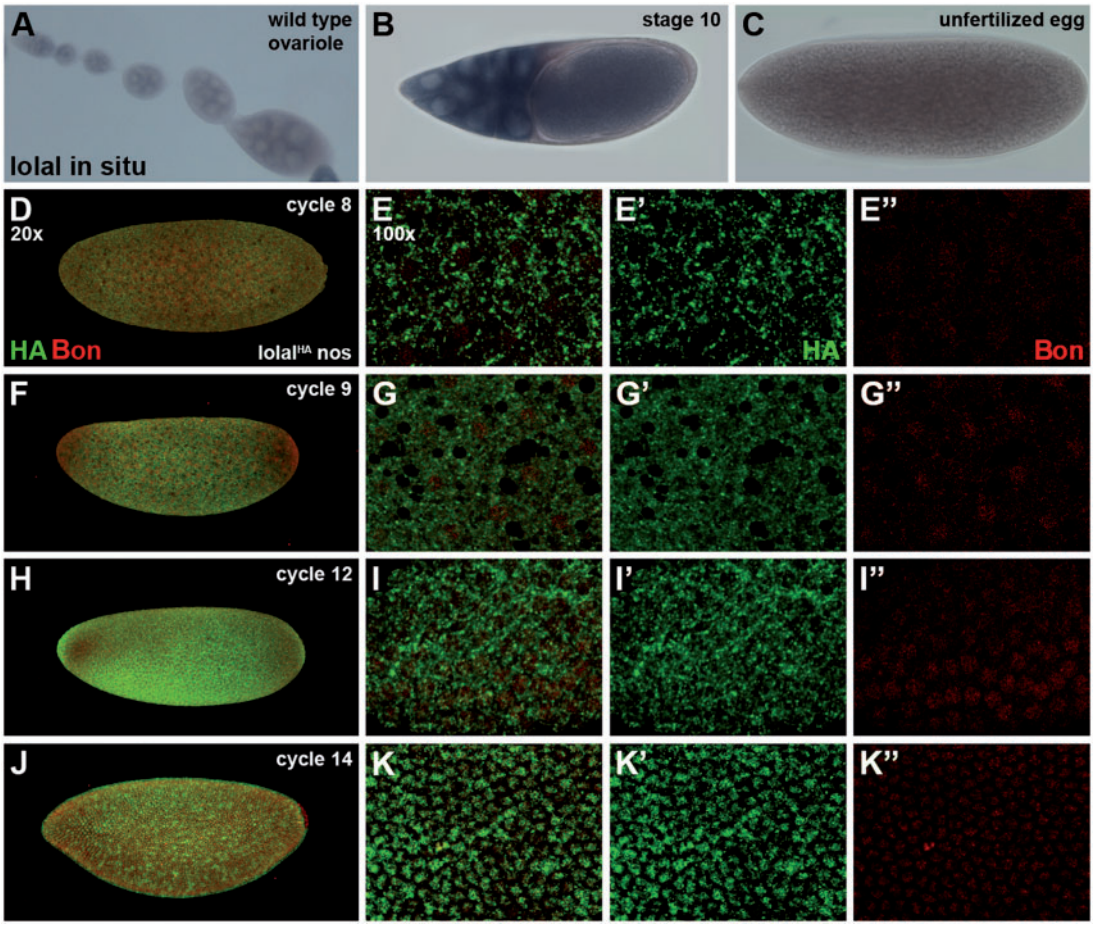

Fig. 3. *lolal* is expressed during oogenesis, is maternally supplied as RNA and protein, and enters nuclei prior to *dpp* transcription. *lolal* maternal RNA expression in wild type revealed via alkaline phosphatase (blue). (*A*) Ovariole, (*B*) Stage 10 egg chamber, and (*C*) Unfertilized egg contain ubiquitous *lolal* RNA. Opposite strand controls are in supplementary fig. S6, Supplementary Material online. (*D-K*) Lolal^{HA} maternal protein expression in embryos shown anterior to the left and dorsal up displaying HA (green) and Bonus (Bon; red) at 20 × (stack) or 100 × (single slices shown as two colors and individual channels). Bonus migrates into nuclei at the maternal to zygotic transition (Wisotzkey et al. 2014) and is employed here as a marker for developmental timing. Unfertilized egg, wild type, and DAPI controls are in supplementary fig. S6, Supplementary Material online. Each row is from the same embryo. (*D*, *E*) Nuclear cycle 8 (Stage 2) embryo has ubiquitously cytoplasmic HA and Bonus. (*F*, *G*) Nuclear cycle 9 (Stage 3) embryo revealing Bonus has begun to concentrate in nuclei whereas HA displays roughly equal concentrations in the cytoplasm and nuclei. (*H*, *I*) Nuclear cycle 12 (latter part of Stage 4) embryo with Bonus completely nuclear whereas HA is still equally present in the cytoplasm and nuclei. (*J*, *K*) Nuclear cycle 14 (Stage 5) embryo with Bonus and HA both completely nuclear.

Supplementary Material online) revealed that half had D/V defects and assays of GLC adult viability did not identify any *lolal* homozygous mutants suggesting the two classes of progeny are as predicted.

dpp transcription in the progeny was then analyzed by fluorescent RNA in situ hybridization assays that included DAPI to identify nuclei for staging. Given reports of stochastic variation in *dpp* expression at this stage (Karim et al. 2012), we employed an unbiased empirical standard of *dpp* pixel intensity to distinguish between the "bottom" and "top" *dpp* expressing groups of embryos corresponding to the two classes of predicted progeny—*lolal* GLC homozygous mutant and *lolal* GLC heterozygous embryos (i.e., computational application of Mendelian ratios to progeny to determine an embryo's genotype). Employing wild-type embryos that were analyzed in parallel and with common reagents as controls, statistical tests were applied to identify differences between the bottom and top classes within *lolal* GLC progeny and within wild-type progeny, as well as differences between the bottom and top *lolal* GLC class and pooled wild-type embryos.

The pixel intensity method easily distinguished two classes of *dpp* expressing embryos with nonoverlapping distributions among *lolal* GLC progeny at early stage 6 (fig. 4, quantitation in supplementary fig. S7, Supplementary Material online). *dpp* was always present in the bottom group, but expression was significantly below the top group ($P = 0.003$). There was no significant difference between the top and bottom groups of wild-type progeny ($P = 0.151$). The *lolal* GLC bottom group was also significantly below wild type ($P = 0.001$), whereas *dpp* expression in the top group of *lolal* GLC progeny was indistinguishable from wild type ($P = 0.785$). Our interpretation is that *lolal* GLC homozygous mutant embryos are the bottom group with reduced expression and heterozygous mutants are the top group since the top group's expression matches wild type. The data show a statistically significant

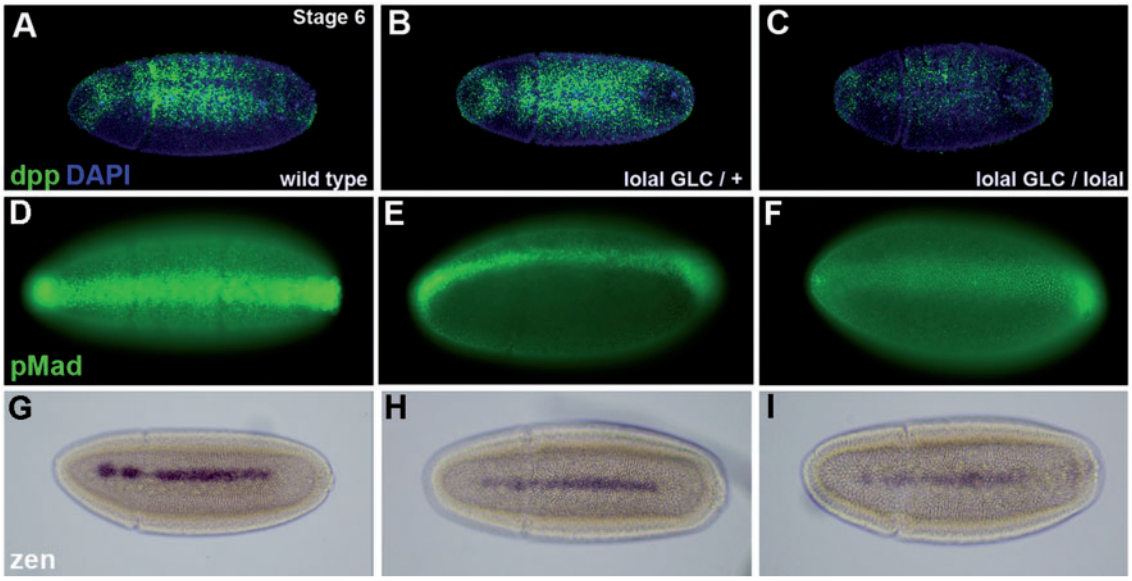

Fig. 4. Loss of maternal and zygotic *lolal* significantly reduces *dpp* and *zen* transcription as well as a pMad expression at stage 6. Stage 6 embryos with anterior to the left and dorsal up. Left column shows wild type embryos stained side-by-side with *lolal* embryos. Middle column shows heterozygous $lolal^{1122}$ germline clone (GLC) embryos with paternal rescue via wild-type *lolal* on the balancer chromosome (lolal GLC/+). Right column shows homozygous *lolal* mutant GLC embryos with $lolal^{1722}$ on the paternal chromosome (lolal GLC/lolal). Detailed methods and quantitative data in supplementary fig. S7, Supplementary Material online. (*A*–*C*) Embryos in dorsal view analyzed by confocal microscopy for *dpp* RNA (green) and DAPI (nuclei; blue). The homozygous GLC embryo contains significantly reduced *dpp* transcription. (*D*–*F*) Embryos in dorsal view analyzed by confocal microscopy for pMad expression (green). The homozygous GLC embryo contains significantly reduced pMad expression. (*G*–*I*) Embryos in dorsal view displaying the narrow dpp-dependent stripe of *zen* RNA analyzed by light microscopy and alkaline phosphatase staining (blue). The homozygous GLC embryo contains significantly reduced *zen* transcription.

reduction in *dpp* transcription intensity in *lolal* GLC homozygous mutants. We conclude that maternal and zygotic *lolal* are each necessary and sufficient for proper *dpp* transcription since the phenotype is visible only in the absence of both.

Consistent with the reduction in *dpp* transcription, the pixel intensity method easily distinguished two classes of pMad expressing embryos with nonoverlapping distributions among *lolal* GLC progeny at early stage 6 (fig. 4, quantitation in supplementary fig. S7, Supplementary Material online). pMad was always present in the bottom group but expression intensity was significantly below the top group ($P = 0.002$). There was no significant difference between the top and bottom groups of wild-type progeny ($P = 0.220$). The *lolal* GLC bottom group was also significantly below wild type ($P = 0.004$), whereas pMad expression in the top group of *lolal* GLC progeny was indistinguishable from wild type ($P = 0.992$). The data show a statistically significant reduction in pMad expression intensity in *lolal* GLC homozygous mutant embryos.

Although frequently employed as an on/off measure, pMad is known to be temporally highly dynamic and moderately variable between embryos of the same age. This makes it less reliable as a quantitative readout (Umulis et al. 2010). A more sensitive indicator of Dpp D/V signaling is the narrow dorsal stripe of *zen* expression at stage 6, a direct transcriptional target of pMad (Rushlow et al. 1987). We applied the quantitative approach to examine the pixel area of *zen* transcription (fig. 4, quantitation in supplementary fig. S7, Supplementary Material online). For *zen*, the pixel area is more relevant than pixel intensity because *zen* expressing cells become the amnioserosa whereas the adjacent nonexpressing cells become the dorsal ectoderm (Rusch and Levine 1997).

Consistent with the reduction in *dpp* transcription and pMad expression, the pixel intensity method easily distinguished two classes of *zen* expressing embryos with nonoverlapping distributions among *lolal* GLC progeny at early stage 6 (fig. 4, quantitation in supplementary fig. S7, Supplementary Material online). *zen* was always present in the bottom group but expression was significantly below the top group ($P = 0.005$). There was no significant difference between the top and bottom groups of wild-type progeny ($P = 0.083$). The *lolal* GLC bottom group was also below wild type ($P = 0.001$), whereas *zen* transcription in the top group was indistinguishable from wild type ($P = 0.131$). The data show a statistically significant reduction in *zen* expression area in *lolal* GLC homozygous mutants. The reduction in *dpp* transcription leading to decreased pMad and *zen* expression in *lolal* homozygous GLC mutant embryos provides a mechanistic explanation for *lolal* dominant maternal enhancement of *dpp*.

The fact that *dpp*, pMad, and *zen* were always present but at significantly reduced levels in *lolal* GLC homozygous mutants at stage 6 suggested a defect in maintenance of *dpp* transcription rather than initiation. To determine if *lolal* GLC homozygous mutants display a defect in the initiation of *dpp* transcription at stage 5, we examined *lolal* GLC embryos at mid and late-stage 5. This is when the *dpp*-dependent pMad dorsal stripe first becomes visible and then strengthens. The

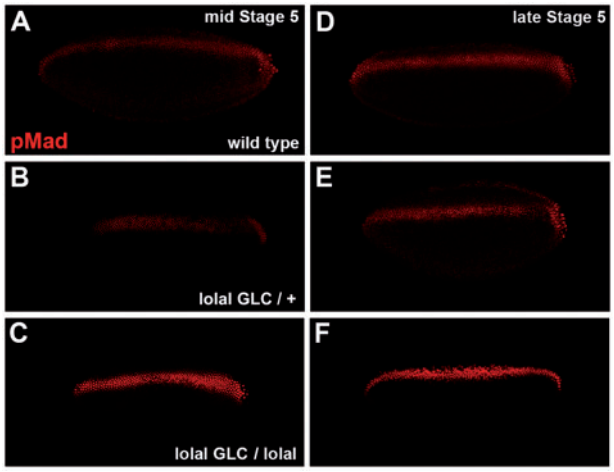

FIG. 5. Loss of maternal and zygotic *lolal* significantly increases pMad expression at stage 5. Mid and late-stage 5 embryos, in the left and right column respectfully, with anterior to the left and dorsal up. Top row contains wild type embryos stained side-by-side with *lolal* embryos. Middle row shows heterozygous $lolal^{1122}$ GLC embryos with paternal rescue via wild type *lolal* on the balancer chromosome (lolal GLC/+). Bottom row shows homozygous $lolal^{1122}$ GLC embryos with $lolal^{1722}$ on the paternal chromosome (lolal GLC/lolal). Detailed methods and quantitative data in supplementary fig. S8, Supplementary Material online. (*A*–*C*) Midstage 5 embryos in dorsal view analyzed by confocal microscopy for pMad expression (red). The homozygous GLC embryo (lolal GLC/lolal) contains significantly increased pMad expression. (*D*–*F*) Late stage 5 embryos analyzed similarly. The homozygous GLC embryo (lolal GLC/lolal) also contains significantly increased pMad expression.

pixel intensity method easily distinguished two classes of pMad expressing embryos with nonoverlapping distributions among *lolal* GLC progeny at both time points (fig. 5, quantitation in supplementary fig. S8, Supplementary Material online). pMad was always present in the bottom group at both times but expression was significantly below the top group (midstage $P = 0.002$; late-stage $P = 0.031$). There was no significant difference at either time between the top and bottom groups of wild type progeny (midstage $P = 0.258$; late-stage $P = 0.175$). The lolal top group was significantly above wild type (midstage $P = 0.002$; late-stage $P = 0.007$), whereas pMad expression in the bottom group was indistinguishable from wild type (midstage $P = 0.566$; late-stage $P = 0.809$). Our interpretation is that *lolal* GLC homozygous mutant embryos are the top group with increased pMad expression and *lolal* heterozygous mutants are the bottom group since the bottom group's expression matches wild type. The mid and late-stage 5 stage data show a statistically significant increase in pMad expression intensity in *lolal* GLC homozygous mutants.

The initial increase in Dpp signaling revealed by the mid and late-stage 5 pMad data together with the subsequent decrease in *dpp* transcription, pMad, and *zen* expression at stage 6 strongly supports our initial thought that *lolal* GLC homozygous mutants have a defect in *dpp* transcription maintenance and not *dpp* transcription initiation. In a final GLC assay, we tested the possibility that *lolal* influences the transcription of other genes in D/V patterning by examining Twist (stage 6), *short gastrulation* (late stage 5), and *zen* (early stage 5—the wide dorsal stripe that is independent of Dpp signaling). For each gene, the two classes of *lolal* GLC progeny were not significantly different from each other nor was either class significantly different from wild type (supplementary fig. S9, Supplementary Material online). This implies that *lolal* function in D/V patterning may be specific to *dpp* transcription, though this conclusion requires additional verification. Overall, from the GLC data, we conclude that *lolal* does not affect *dpp* transcript initiation but instead is required for maintenance of proper *dpp* transcription levels.

Lolal Is a New BTB Domain Protein

Lolal is a small protein of 123 amino acids. Eighty-six residues are devoted to a BTB domain. BTB (also known as POZ) is a well-established homo- and hetero-multimerization domain (Bonchuk et al. 2011). The BTB domain is present in a very large family of proteins, with members in eukaryotes and prokaryotes characterized by rapid birth-and-death evolution (Domman et al. 2014). BTB proteins are highly diverse with N- and C-terminal extensions containing other domains (Stogios et al. 2005). In eukaryotes, BTB domains are often found in chromatin proteins (Bonchuk et al. 2011). Upstream of the BTB domain 27 residues form a Pipsqueak (Psq) domain found in Lolal's closest relatives but that has no known function (Siegmund and Lehmann 2002). To better understand Lolal origins, a phylogenetic tree containing fly, nematode, and human proteins with BTB domains similar to Lolal was constructed (fig. 6).

The Lolal family tree has two subfamilies and the Lolal subfamily has two branches. The Lolal branch contains 11 fly proteins, including the well-known chromatin/epigenetic protein Trithorax-like (Trl; a Zinc-finger protein also known as GAGA factor) as part of the Lolal group. The Lolal branch contains a single human protein, BTBD18 (hCG1730474; Alonso et al. 2010) that does not contain a Zinc-finger but has a recognizable Psq domain. BTBD18 was identified in a single patient as a fusion with the *myeloid/lymphoid leukemia* gene but has no known function. The sister to the Lolal branch contains 11 human proteins and a single fly protein. The asymmetric topology of these branches is consistent with previously noted lineage-specific expansions in the BTB family (Aravind and Koonin 1999). Of the 24 proteins in the Lolal subfamily, 19 contain a DNA-binding Zinc finger domain whereas the other primary subfamily is composed of non–DNA-binding Math/Bath and Kelch domain proteins.

Overall, the tree topology suggests that the common ancestor of the Lolal subfamily contained Zinc-finger, Psq, and BTB domains. Then, in the Lolal branch the arthropod, but not the vertebrate lineage, experienced multiple gene duplications with the Zinc-finger lost in a few instances including Lolal. The Lolal cluster, consisting of Lolal and its closest relatives Tramtrack (Ttk), Lola, and Modifier of mdg4 (Mmd4), is the most distant from HsBTBD18 indicating that it resulted from the most recent arthropod duplications. This inference that Lolal is arthropod-specific is supported by unsuccessful searches for Lolal cluster sequences in other vertebrate

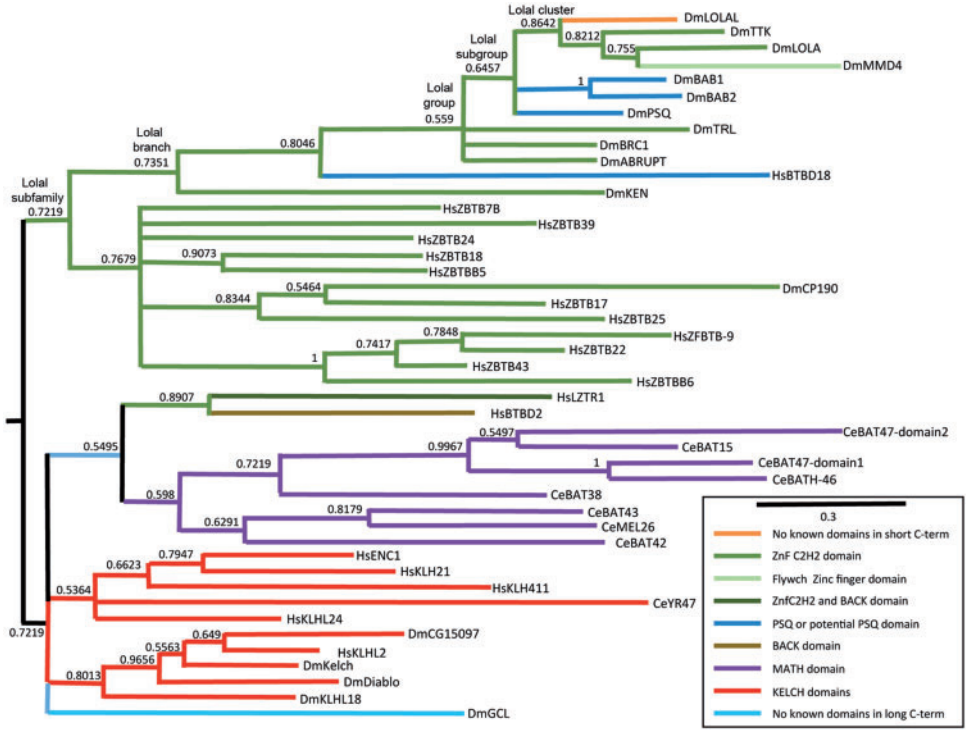

Fig. 6. Lolal is a new arthropod-specific BTB protein. Bayesian tree displaying 45 human (Hs), fly (Dm), and nematode (Ce) BTB domain proteins. Twenty-three proteins (Lolal subfamily) were selected due to the similarity of their BTB domain to Lolal. The other 21 proteins (bottom subfamily) contain Math/Bath or Kelch domains in addition to a BTB domain to provide a robust outgroup and allow the tree to be midpoint rooted. Lolal has no close vertebrate relatives indicating it is a new family member born after the arthropod-vertebrate divergence. Accession numbers are in supplementary table S8a, Supplementary Material online. Nodes defining tree features associated with Lolal are named. A scale bar showing amino acid substitutions per site is present. Colors of branches indicate the presence of additional functional domains as described. Posterior probabilities above 0.5 are shown. The alignment contained 77 informative positions. As described in the Materials and Methods, for alignments between 50 and 100 informative characters posterior probabilities $\geq$0.75 should be considered statistically significant.

genomes and the genomes of vertebrate siblings the sea urchin and tunicate.

The phyla Arthropoda consists of four subphyla—insects, crustaceans, chelicerates (mites/spiders), and myriapods (centipedes/millipedes). Phylogenetic studies indicate that the first to diverge were the chelicerates (543 million years ago [Mya]) then the myriapods (539 Mya) with insects and crustaceans separating 470 Mya (Rota-Stabelli et al. 2013). Utilizing this information as a scaffold, additional analyses such as reciprocal BLASTs, amino acid conservation frequency, and intron–exon structure comparisons suggested a serial duplication scenario that matches the topology for the Lolal subgroup: 1) Bab is oldest (present in all four subphyla), 2) Bab generated Ttk (present in insects and chelicerates but lost in crustaceans), 3) Ttk generated Lolal (present in insects and crustaceans), 4) Bab later generated Psq (present in insects and crustaceans), 5) Ttk later generated Mmd4 (only present in insects but has a longer branch than Lola), and 6) Mmd4 generated Lola (only present in insects).

The specificity of Lolal to insects and crustaceans is shown in a representative tree of Lolal homologs (four insect and five crustacean species; fig. 7). Overall the phylogenetic data shows that Lolal was generated in the arthropod lineage 230 Mya after the arthropod-vertebrate split (700 Mya; Parfrey et al. 2011). Although not the newest gene in its subgroup, it is newer than any known *Drosophila* gene in D/V axis formation as all of the others have vertebrate homologs (e.g., Dorsal, Sog, Twist, Dpp, Mad, and Medea).

Discussion

dpp Transcription in D/V Patterning

The genetic screen that pointed us to *lolal* also identified a second deletion, *Df(3L)66C-G28*, displaying dominant maternal enhancement. Employing the same candidate gene approach, we determined that *moleskin* is the dominant maternal enhancer of *dpp* in that deletion (supplementary fig. S10, Supplementary Material online). *moleskin* is a nuclear importer for Mad that was not previously implicated in D/V patterning (Xu et al. 2007). These two discoveries, 20 years after the identification of *Mad* and *Medea* utilizing the same enhancement screen, reinforce the value of genetic analyses in *Drosophila* as the premier method for gene discovery.

Genetic screens have also identified the maternal transcription factors Zelda and Stat92E as general activators of early zygotic genes including *dpp*, *sog*, *zen*, and *twist* (Liang et al. 2008; Tsurumi et al. 2011). Lolal differs from Zelda/Stat92E in three ways: 1) *lolal* displays dominant maternal enhancement of *dpp* mutants whereas Stat92E does not, 2) *dpp* transcription initiates but goes awry in *lolal* GLC homozygous embryos whereas it does not initiate in Zelda or

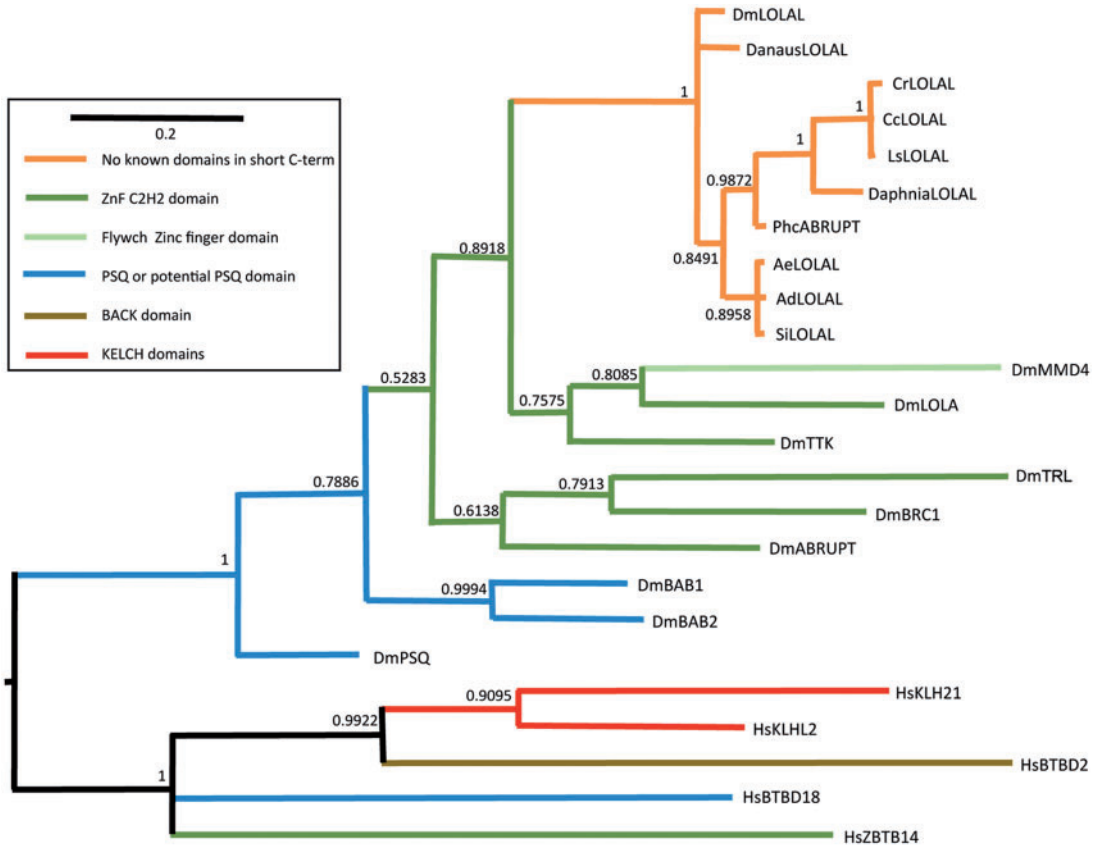

Fig. 7. Lolal is only present in insects and crustaceans. Bayesian tree of 24 proteins containing BTB domains similar to the Lolal BTB domain. These include the nine fly (Dm) proteins in the Lolal group of Fig. 6 (blue and green branches), plus nine insect, and crustacean Lolal homologs identified by BLAST (orange branches) The others are human (Hs) proteins, one from each of the five branches from Fig. 6. Pairwise alignments revealed that PhcABRUPT is misnamed as its BTB domain is 93% identical to Lolal's and it does not contain a Zinc-finger like DmABRUPT (green branch). Accession numbers are in supplementary table S8b, Supplementary Material online. The scale bar shows the number of amino acid substitutions per site. Colors of branches indicate the presence of additional functional domains as described. Posterior probabilities above 0.5 are shown. The alignment contained 89 informative positions. As described in the Materials and Methods, for alignments of between 50 and 100 informative characters posterior probabilities $\geq$0.75 should be considered statistically significant.

Stat92E GLC homozygous embryos, and 3) *sog*, early *zen*, and Twist expression are unaffected in *lolal* GLC homozygous embryos whereas they do not initiate in Zelda or Stat92E GLC homozygous embryos.

Mechanistically, Lolal may be needed to regulate *dpp* transcription because activation of early zygotic genes in *Drosophila* requires the combinatorial activity of transcription factors and chromatin proteins (Darbo et al. 2013; Sandler and Stathopoulos 2016). Chromatin proteins have been generally separated into the Polycomb group of repressors and the Trithorax group of activators though there are several that can perform both roles such as the Lolal group member Trl (Schuettengruber et al. 2007). Trl functions by influencing the placement of a methyl group on Histone H3 Lysine 9 (closed chromatin) or Lysine 4 (open chromatin) thereby modulating chromatin accessibility [reviewed in Kim and Kim (2012)].

The most prominent chromatin proteins active during the maternal to zygotic transition are Trl and the Lolal cluster member Ttk. Lolal has been shown to physically interact with Trl, to co-localize with Trl on larval salivary gland chromosomes and to co-localize with Trl in regions of actively transcribing chromatin in an embryo-derived cell line (Faucheux et al. 2003; Mishra et al. 2003; Filion et al. 2010). In vitro Lolal forms heteromeric complexes with its subgroup relatives Ttk, Mmd4, and Psq (Bonchuk et al. 2011). Functionally, these four proteins form a genetic network that regulates ovariole number in *Drosophila* (Bartoletti et al. 2012).

Our hypothesis is that Lolal, with its epigenetic partner Trl, modifies chromatin near the cycle 10 *dpp* enhancers following Zelda/State92E activation of transcription. Lolal's epigenetic role is to maintain proper levels of *dpp* transcription over the next four nuclear cycles as the extracellular Dpp D/V morphogen gradient is established. Two pieces of additional evidence support this idea. First, dominant maternal enhancement assays with mutations in Lolal's closest relatives revealed a strong effect (supplementary table S1, Supplementary Material online) of a deletion allele of *pipsqueak* that removes Exon1A (*Df(2R)12*; Weber et al. 1995). *pipsqueak* has a maternal contribution and its earliest embryonic expression is dorsal-specific (Weber et al. 1995) putting it in a position to partner with Lolal in the regulation of *dpp*. Further, Pipsqueak functions are essential for sequence-

specific targeting of epigenetic complexes (Huang et al. 2002). Second, sequences in the *dpp* second intron are responsible for the cycle 10 initiation of *dpp* transcription (Huang et al. 1993; Jackson and Hoffmann 1994). An alignment of four *Drosophila* species revealed numerous conserved Zelda, Stat92E, and Trl binding sites in this intron supporting a role for epigenetic complexes in the modulation of *dpp* transcription.

New Gene Evolution in D/V Patterning

Studies of new genes in *Drosophila* showed that these could quickly become essential for viability, fertility, and behavior (Chen et al. 2013; Long et al. 2013). Indispensability for fertility and behavior results from the incorporation of new genes into existing pathways. A prediction of these studies is that the assimilation of new genes into developmental pathways underlies their requirement for viability. To gain insight into the evolutionary mechanisms behind the generation of new genes, we are currently comparing the expression patterns and upstream sequences of Lolal group proteins with the goal of correlating changes in expression with changes in transcription factor binding sites.

The architecture of D/V patterning, and the Dpp/BMP pathway at its center, is among the most highly conserved processes in Bilaterian development. This taxon is also called Eumetazoa and it originated roughly one billion years ago (bya; Kumar and Hedges 2011). Organisms as diverse as planarians and humans employ a common set of signaling molecules in a common format, albeit inverted in some cases (De Robertis and Sasai 1996). The Dpp/BMP pathway has other functions in development and is older than Bilateria. A complete Dpp/BMP pathway is present in *Nematostella vectensis* (a diploblast with two germ layers that originated 1.1 bya; Putnam et al. 2007). Individual members of families in the Dpp/BMP pathway including ligands, receptors, and Smads are found in all Metazoans including sponges [*Amphimedon queenslandica* originated 1.3 bya; reviewed in Konikoff et al. (2008)].

Although D/V patterning is conserved, its individual proteins are always under selective pressure. We recently showed in the vertebrate D/V program that a new gene can provide a selective advantage and become incorporated into this process. Our analysis of the ubiquitin ligases targeting vertebrate Smad4 and its fly homolog Medea revealed that a new vertebrate protein belonging to the RING class of ligases (TIF1-γ/TRIM33) replaced an older HECT class ligase (Nedd4) that performs this job in flies and presumably in the arthropod-vertebrate common ancestor. That data demonstrated that the vertebrate D/V program was not simply conserved since its divergence from flies, but has evolved by incorporating new genes (Wisotzkey et al. 2014).

The results for Lolal strongly complement that for TIF1-γ/TRIM33 with this new gene incorporated into the arthropod D/V program. Although certainly possible that Lolal replaced an older gene that performs epigenetic functions in D/V patterning upstream of *dpp* transcription in the common ancestor of arthropods and vertebrates, there are no known genes upstream of BMP in vertebrate D/V axis formation to guide us. Nevertheless, employing the Nedd4 and TIF1-γ/TRIM33 replacement scenario as a reference, data reported here suggest that the function performed by Lolal (epigenetic marker) is essential to vertebrate D/V patterning and that a complex containing proteins similar to Lolal and Trl fulfill this role. Among the Trl top BLAST hits in mammals is MIZ-1, which we propose as a candidate BMP transcription regulator in D/V axis formation. MIZ-1 forms multimers with the proto-oncogene BCL6 and the complex regulates the transcription of cyclin-dependent kinase inhibitor p21 to promote cell proliferation in adult B cells (Phan et al. 2005). Taken together, the phylogenetic data for Lolal and TIF1-γ/TRIM33 shows that the D/V patterning program shared by all Bilateria contains highly conserved features such as Dpp/BMP ligands, receptors, and Smads as well as dynamic features such ubiquitin ligases and chromatin proteins that are influenced by the assimilation of new genes.

Overall, we report that Lolal is the first maternal protein identified with a role in *dpp* D/V transcriptional maintenance. Equally important corollaries are that Lolal and the epigenetic protein Trl are essential for Dpp D/V signaling and that the architecture of the Dpp D/V pathway evolved in the arthropod lineage after the separation from vertebrates via the incorporation of new genes such as *lolal*.

Materials and Methods

Flies

Mutants are *Df(2R)Pcl-11B* (Nicholls and Gelbart 1998), *Df(2R)12* (*psq*; Weber et al. 1995), *Df(3L)bab*^{Ar07} (deletion of *bab1* and *bab2*; Couderc et al. 2002), *dpp*^{e87}, *dpp*^{hr4}, *dpp*^{hr27}, *dpp*^{hr56} (St. Johnston et al. 1990), *lola*^{ORE76} (Horiuchi et al. 2003), *P{EP}lolal*^{G9603} (Bellen et al. 2004), *P{lacW}lolal*^{K02512} (Török et al. 1993), *lolal*^{1122}, and *lolal*^{1722} (this work), *Mad*^{12} and *Med*^{15} (Stinchfield et al. 2012), *modifier of mdg4*^{T6} (*mmd4*; Soltani-Bejnood et al. 2007), *Trl*^{R67} (Farkas et al. 1994), and *ttk*^{1e11} (Xiong and Montell 1993). Transgenic strains are *dpp*-lacZ-BS3.0 (Blackman et al. 1991), *P{lacW}brk*^{38} (*brinker*-lacZ; Minami et al. 1999), *Trl*^{EY04024} (Bellen et al. 2011), nos.Gal4:VP16-MVD1, UASP.GFP-αTub84B, UASP.Med^{wt}, and UASP.Med^{K738R} (Stinchfield et al. 2012), UASP.Sax* (Xie and Spradling 1998) and UASP.Tkv* (Casanueva and Ferguson 2004). Balancers and GLC strains are in Flybase (Marygold et al. 2013).

Genetics

Assays for adult viability, dominant maternal enhancement, stage of lethality, transgenic rescue, and zygotic lethality were conducted as described (Stinchfield et al. 2012). Germline clone (GLC) females were generated with *FRTG13 lolal*^{1122} as described (Wisotzkey et al. 2014). GLC females were mated to *lolal*^{1722} heterozygous males to assay *lolal* homozygous embryos (*lolal*^{1122}/*lolal*^{1722}) and paternally rescued heterozygous embryos. Homozygous GLC embryos were identified by quantitative comparison with wild type. Pixel intensity plots reflecting *dpp*, sog, *zen* (stage 5), pMad, or Twist expression were created from single channel images in ImageJ (Schneider et al. 2012). Mean pixel intensity was obtained from areas of interest drawn on the embryo. The relative mean pixel

intensity was calculated by subtracting the mean pixel intensity of background (lateral region) from that of the expression domain, thus normalizing expression for each embryo prior to statistical analysis. For *zen* at stage 6, the pixel area was obtained by calculating the number of pixels within a domain encompassing all cells expressing *zen*. Pixel intensity and area values were imported into Excel and graphed. Extensive efforts were employed to minimize variation in technique with wild-type and *lolal* GLC embryos stained side-by-side, on the same day, using a similar number of embryos, the same probe, the same antibody, the same wash solutions, and imaged on the same day with the same settings on our only confocal. In the image analysis, only wild type and *lolal* GLC embryos from the same date were compared. Wing disk clones of *FRTG13 lolal*^{1122} were generated by standard methods, marked by the absence of *GFP* and analyzed as described (Quijano et al. 2011).

Embryos

Cuticle preparations were as described and cuticle scoring employed standard criteria (e.g., Stinchfield et al. 2012). Fluorescent RNA in situ hybridization followed by TSA-488 (Molecular Probes) was utilized to visualize *dpp* as described (Ray et al. 1991; Nagaso et al. 2001). Alkaline phosphatase RNA in situ hybridization for *sog, zen*, and *lolal* were conducted as described (Künnapuu et al. 2014). Nuclei were visualized directly with DAPI (Sigma). Primary antibodies were: Bonus-GP37 (Beckstead et al. 2001), Digoxigenin (Zymed), Dorsal (DSHB-7A4), HA-3F10 (Roche), Hindsight (DSHB-1G9), LacZ (Organon Teknika), pSmad (Epitomics), dSRF (Marenda et al. 2004), and Twist (Roth et al. 1989). Secondary antibodies were: donkey α-sheep-HRP (for TSA; Life Technologies), or AlexaFluor 488, 546 or 633 goat α-mouse, α-rabbit, α-rat or α-guinea pig (Life Technologies). Embryos were fixed after 4–6 h, antibody labeled and imaged as described (Quijano et al. 2011).

Molecular Biology

UAST.Lolal was generated by cloning a SpeI—XhoI fragment from cDNA *pOT2-LD14505* (Berkeley Drosophila Genome Project) into the NheI—XhoI sites of pUAST2. PCR products of the coding region from this clone were inserted into two Drosophila Gateway vectors: pPW to create UASP.Lolal or pPWH to create UASP.Lolal^{HA} (Drosophila Genomics Resource Center) followed by recombination into UASP. Primers for Gateway cloning were:

UASP.Lolal: Forward 5′-CACCATGATGTCGTCGGATCAACAG-3′
Reverse 5′-TCAACCTTCCCGCTTTATCG-3′
UASP.Lolal^{HA}: Forward 5′-CACCATGATGTCGTCGGATCAACAG-3′
Reverse 5′-ACCTTCCCGCTTTATCGAAC-3′

A *lolal* RNA in situ probe was generated by PCR via a primer bearing a T7 sequence overhang. Antisense RNA was then synthesized with T7 polymerase. Primers for PCR were:

Forward 5′-TAATACGACTCACTATAGGGCGAACTGGGTGTCTCTGCGAGG-3′
T7promoter
Reverse 5′-GACCTCGTTCCGTCACCTGCG-3′

For dsRNA, pairs of primers containing T7 sequence overhangs were designed for PCR. These products were templates for dsRNA synthesis via the MEGAscript T7 kit (Applied Biosystems). ds-*punt* and ds-*lacI* are as described (Zeng et al. 2014). Primers for two distinct ds-*lolal* RNAs:

1-F: 5′-TAATACGACTCACTATAGGGAGAAGC GCTACTGGAGGAGAACCC-3′
1-R: 5′-TAATACGACTCACTATAGGGAGAACCTTCCCGCTTTATCGA ACTGGG-3′
3′-F: 5′TAATACGACTCACTATAGGGAGAAAATACATAATAAATAAC AACAACCAA-3′
3′-R: 5′-TAATACGACTCACTATAGGGAGATGGCCTCCACCTCTACTTT ACAGGC-3′

One assay for Dpp signal transduction employed *Drosophila* S2 cells that were transfected with Flag-Mad and incubated with dsRNA (Ross et al. 2001). After 3 days, these cells were incubated with Dpp for 3 h. Dpp signaling in these cells was measured by western blots with the mouse α-Flag M2 (Sigma) and rabbit α-pMad. These antibodies were detected with α-mouse-680 and α-rabbit-800 (LI-COR) and analyzed with an Odyssey Infrared Imaging System as described (Künnapuu et al. 2014). A second Dpp signaling assay utilized S2 cells transfected with dsRNA, Dad13-firefly plasmid, and *Renilla* luciferase plasmid. Five days after transfection, the cells were incubated with Dpp for 26 h. Cells were lysed and analyzed using a dual luciferase reporter assay system (Promega) with reporters as described (Weiss et al. 2010; Matsuda et al. 2013).

Phylogenetics

For figure 6, sequences most similar to Lolal were identified by BLAST from among the 83 BTB proteins in *D. melanogaster*, 181 in *Caenorhabditis elegans* and 183 in *Homo sapiens* (BTB domain database; btb.uhnres.utoronto.ca). For figure 7, a second set of sequences most similar to Lolal regardless of species was constructed. Analyses in arthropod subphyla employed these databases: *Daphnia pulex, Strigamia maritime, Tetranychus urticae* (Ensembl Genomes), *Metaseiulus occidentalis* (NCBI Refseq), and *Ixodes scapularis* (Vectorbase). Alignments were created with default settings in Clustal Omega at the EMBL-EBI website (ebi.ac.uk/Tools/msa/clustalo) and trees were created in MrBayes 3.2 as described (Wisotzkey et al. 2014). The mixed amino acid model was selected and in both cases the WAG model was employed (Whelan and Goldman 2001). Generations were 100,000 for figure 6 and 600,000 for figure 7 with a sample frequency of 100 and burn-in of 0.25. For trees with more than 150 informative positions a posterior probability of 0.95 is considered statistically significant but simulation studies (Alfaro et al. 2003) of alignments with 50–100 positions revealed that the true tree contained branches with posterior probabilities of 0.65 (50 positions) and 0.85 (100 positions). Thus, for our trees of 77 (fig. 6) and 89 (fig. 7) informative positions, we consider probabilities $\geq$0.75 to be statistically significant.

Supplementary Material

Supplementary figures S1–S10 and tables S1–S8 are available at *Molecular Biology and Evolution* online (http://www.mbe.oxfordjournals.org/).

Acknowledgments

This paper is dedicated to the memory of our mentor and friend Bill Gelbart, in whose lab dominant maternal enhancement screens with *dpp* mutations originated. We thank H. Bellen, E. Ferguson, M. Leptin, G. Pyrowolakis, P. ten Dijke, Berkeley Drosophila Genome Project, Bloomington Stock Center, Drosophila Genome Resource Center, and Iowa Hybridoma Bank for reagents. We thank C. Konikoff, J. Künnapuu, and J. Seemann for assistance with data collection. This work was supported by the Academy of Finland to O.S., National Institutes of Health grants to S.J.N. (GM099650 and NS072128), and a United States – Israel Binational Science Foundation grant to S.J.N. (2013380).

References

Alfaro ME, Zoller S, Lutzoni F. 2003. Bayes or bootstrap: a simulation study comparing the performance of Bayesian Markov chain Monte Carlo sampling and bootstrapping in assessing phylogenetic confidence. *Mol Biol Evol*. 20:255–266.

Alonso CN, Meyer C, Gallego MS, Rossi JG, Mansini AP, Rubio PL, Medina A, Marschalek R, Felice MS. 2010. BTBD18: a novel MLL partner gene in an infant with acute lymphoblastic leukemia and inv(11)(q13;q23). *Leuk Res*. 34:e294–e296.

Aravind L, Koonin EV. 1999. Fold prediction and evolutionary analysis of the POZ domain: structural and evolutionary relationship with the potassium channel tetramerization domain. *J Mol Biol*. 285:1353–1361.

Bartoletti M, Rubin T, Chalvet F, Netter S, Dos Santos N, Poisot E, Paces-Fessy M, Cumenal D, Peronnet F, Pret A, et al. 2012. Genetic basis for developmental homeostasis of germline stem cell niche number: a network of Tramtrack-Group nuclear BTB factors. *PLoS One* 11:e49958.

Beckstead R, Ortiz JA, Sanchez C, Prokopenko SN, Chambon P, Losson R, Bellen HJ. 2001. *Bonus*, a *Drosophila* homolog of TIF1 proteins, interacts with nuclear receptors and can inhibit βFTZ-F1-dependent transcription. *Mol Cell* 7:753–765.

Bellen H, Levis R, Liao G, He Y, Carlson JW, Tsang G, Evans-Holm M, Hiesinger PR, Schulze K, Rubin G, et al. 2004. The BDGP gene disruption project: single transposon insertions associated with 40% of *Drosophila* genes. *Genetics* 167:761–781.

Bellen HJ, Levis RW, He Y, Carlson JW, Evans-Holm M, Bae E, Kim J, Metaxakis A, Savakis C, Schulze K, et al. 2011. The Drosophila gene disruption project: progress using transposons with distinctive site specificities. *Genetics* 188:731–743.

Bier E, De Robertis EM. 2015. BMP gradients: a paradigm for morphogen-mediated developmental patterning. *Science* 348:1433.

Blackman RK, Sanicola M, Raftery LA, Gillevet T, Gelbart WM. 1991. An extensive 3′ cis-regulatory region directs the imaginal disk expression of decapentaplegic, a member of the TGF-β family in *Drosophila*. *Development* 111:657–666.

Bonchuk A, Denisov S, Georgiev P, Maksimenko O. 2011. *Drosophila* BTB/POZ domains of ttk group can form multimers and selectively interact with each other. *J Mol Biol*. 412:423–436.

Casanueva MO, Ferguson EL. 2004. Germline stem cell number in the *Drosophila* ovary is regulated by redundant mechanisms that control Dpp signaling. *Development* 131:1881–1890.

Chen S, Krinsky BH, Long M. 2013. New genes as drivers of phenotypic evolution. *Nat Rev Genet*. 14:645–660.

Couderc J, Godt D, Zollman S, Chen J, Li M, Tiong S, Cramton S, Sahut-Barnola I, Laski FA. 2002. The *bric a brac* locus consists of two paralogous genes encoding BTB/POZ domain proteins and acts as a homeotic and morphogenetic regulator of imaginal development in *Drosophila*. *Development* 129:2419–2433.

Darbo E, Herrmann C, Lecuit T, Thieffry D, van Helden J. 2013. Transcriptional and epigenetic signatures of zygotic genome activation during early *Drosophila* embryogenesis. *BMC Genomics* 14:226.

De Robertis EM, Sasai Y. 1996. A common plan for dorsoventral patterning in Bilateria. *Nature* 380:37–40.

Domman D, Collingro A, Lagkouvardos I, Gehre L, Weinmaier T, Rattei T, Subtil A, Horn M. 2014. Massive expansion of ubiquitination-related gene families within the *Chlamydiae*. *Mol Biol Evol*. 11:2890–2904.

Farkas G, Gausz J, Galloni M, Reuter G, Gyurkovics H, Karch F. 1994. The Trithorax-like gene encodes the Drosophila GAGA factor. *Nature* 371:806–808.

Faucheux M, Roignant JY, Netter S, Charollais J, Antoniewski C, Théodore L. 2003. *batman* interacts with polycomb and trithorax group genes and encodes a BTB/POZ protein that is included in a complex containing GAGA factor. *Mol Cell Biol*. 23:1181–1195.

Filion G, van Bemmel JG, Braunschweig U, Talhout W, Kind J, Ward LD, Brugman W, de Castro I, Kerkhoven RM, Bussemaker HJ, et al. 2010. Systematic protein location mapping reveals five chromatin types in *Drosophila*. *Cell* 143:212–224.

Fisher WW, Li JJ, Hammonds AS, Brown JB, Pfeiffer BD, Weiszmann R, MacArthur S, Thomas S, Stamatoyannopoulos JA, Eisen MB, et al. 2012. DNA regions bound at low occupancy by transcription factors do not drive patterned reporter gene expression in *Drosophila*. *Proc Natl Acad Sci U S A*. 109:21330–21335.

Horiuchi T, Giniger E, Aigaki T. 2003. Alternative trans-splicing of constant and variable exons of a *Drosophila* axon guidance gene *lola*. *Genes Dev*. 17:2496–2501.

Huang DH, Chang YL, Yang CC, Pan IC, King B. 2002. *pipsqueak* encodes a factor essential for sequence-specific targeting of a polycomb protein complex. *Mol Cell Biol*. 22:6261–6271.

Huang JD, Schwyter DH, Shirokawa JM, Courey AJ. 1993. The interplay between enhancer and silencer elements defines the pattern of *dpp* expression. *Genes Dev*. 7:694–704.

Jackson PD, Hoffmann FM. 1994. Embryonic expression patterns of the *Drosophila dpp* gene: separate regulatory elements control blastoderm expression and lateral ectodermal expression. *Dev Dyn*. 199:28–44.

Karim MS, Buzzard GT, Umulis DM. 2012. Secreted, receptor-associated BMP regulators reduce stochastic noise intrinsic to many extracellular morphogen distributions. *J R Soc Interface*. 9:1073–1083.

Kim J, Kim H. 2012. Recruitment and biological consequences of histone modification of H3K27me3 and H3K9me3. *ILAR J*. 53:232–239.

Konikoff CE, Wisotzkey RG, Newfeld SJ. 2008. Lysine conservation and context in TGF-β and Wnt signaling suggest new targets and general themes for posttranslational modification. *J Mol Evol*. 67:323–333.

Kumar S, Hedges SB. 2011. TimeTree2: species divergence times on the iPhone. *Bioinformatics*. 27:2023–2024.

Künnapuu J, Tauscher PM, Tiusanen N, Nguyen M, Löytynoja A, Arora K, Shimmi O. 2014. Cleavage of the *Drosophila* Screw prodomain is critical for a dynamic BMP morphogen gradient in embryogenesis. *Dev Biol*. 389:149–159.

Liang HL, Nien CY, Liu HY, Metzstein MM, Kirov N, Rushlow C. 2008. Zinc-finger protein Zelda is a key activator of the early zygotic genome in *Drosophila*. *Nature* 456:400–403.

Long M, VanKuren NW, Chen S, Vibranovski MD. 2013. New gene evolution: little did we know. *Annu Rev Genet*. 47:307–333.

Marenda DR, Zraly CB, Dingwall AK. 2004. The *Drosophila* Brahma (SWI/SNF) chromatin remodeling complex exhibits cell-type specific activation and repression functions. *Dev Biol*. 267:279–293.

Marygold SJ, Leyland PC, Seal RL, Goodman JL, Thurmond J, Strelets VB, Wilson RJ, Flybase consortium. 2013. FlyBase: improvements to the bibliography. *Nucleic Acids Res*. 41:D751–D757.

Matsuda S, Blanco J, Shimmi O. 2013. A feed-forward loop coupling extracellular BMP transport and morphogenesis in *Drosophila* wing. *PLoS Genet*. 9:e1003403.

Minami M, Kinoshita N, Kamoshida Y, Tanimoto H, Tabata T. 1999. *brinker* is a target of Dpp that negatively regulates Dpp-dependent genes. *Nature* 398:242–246.

Mishra K, Chopra VS, Srinivasan A, Mishra RK. 2003. Trl-GAGA directly interacts with Lola-like and both are part of the repressive complex of Polycomb group of genes. *Mech Dev*. 120:681–689.

Nagaso H, Murata T, Day N, Yokoyama KK. 2001. Simultaneous detection of RNA and protein by in situ hybridization and immunological staining. *J Histochem Cytochem*. 49:1177–1182.

Nicholls RE, Gelbart WM. 1998. Identification of chromosomal regions involved in *dpp* function in *Drosophila*. *Genetics* 149:203–215.

Parfrey LW, Lahr DJ, Knoll AH, Katz LA. 2011. Estimating the timing of early eukaryotic diversification with multigene molecular clocks. *Proc Natl Acad Sci U S A*. 108:13624–13629.

Phan RT, Saito M, Basso K, Niu H, Dalla-Favera R. 2005. BCL6 interacts with the transcription factor Miz-1 to suppress the cyclin-dependent kinase inhibitor p21 and cell cycle arrest in germinal center B cells. *Nat Immunol*. 6:1054–1060.

Pritchard DK, Schubiger G. 1996. Activation of transcription in *Drosophila* embryos is a gradual process mediated by the nucleocytoplasmic ratio. *Genes Dev*. 10:1131–1142.

Putnam NH, Srivastava M, Hellsten U, Dirks B, Chapman J, Salamov A, Terry A, Shapiro H, Lindquist E, Kapitonov VV, et al. 2007. Sea anemone genome reveals ancestral eumetazoan gene repertoire and genomic organization. *Science* 317:86–94.

Quijano JC, Stinchfield MJ, Newfeld SJ. 2011. Wg signaling via Zw3 and Mad restricts self-renewal of sensory organ precursor cells in *Drosophila*. *Genetics* 189:809–824.

Ray RP, Arora K, Nusslein-Volhard C, Gelbart WM. 1991. The control of cell fate along the dorsal-ventral axis of the *Drosophila* embryo. *Development* 113:35–54.

Ross JJ, Shimmi O, Vilmos P, Petryk A, Kim H, Gaudenz K, Hermanson S, Ekker SC, O'Connor MB, Marsh JL. 2001. Twisted gastrulation is a conserved extracellular BMP antagonist. *Nature* 410:479–483.

Rota-Stabelli O, Daley A, Pisani D. 2013. Molecular timetrees reveal a Cambrian colonization of land and a new scenario for ecdysozoan evolution. *Curr Biol*. 23:392–398.

Roth S, Stein D, Nüsslein-Volhard C. 1989. A gradient of nuclear localization of the dorsal protein determines dorsoventral pattern in the *Drosophila* embryo. *Cell* 59:1189–1202.

Rusch J, Levine M. 1997. Regulation of a *dpp* target gene in the *Drosophila* embryo. *Development* 124:303–311.

Rushlow C, Frasch M, Doyle H, Levine M. 1987. Maternal regulation of *zerknullt*: a homoeobox gene controlling differentiation of dorsal tissue in *Drosophila*. *Nature* 330:583–586.

Sandler JE, Stathopoulos A. 2016. Quantitative single-embryo profile of *Drosophila* genome activation and the Dorsal-Ventral patterning network. *Genetics* 4:1575–1584.

Schneider CA, Rasband WS, Eliceiri KW. 2012. NIH Image to ImageJ: 25 years of image analysis. *Nat Methods*. 9:671–675.

Schuettengruber B, Chourrout D, Vervoot M, Leblanc B, Cavalli G. 2007. Genome regulation by polycomb and trithorax proteins. *Cell* 128:735–745.

Sekelsky JJ, Newfeld SJ, Raftery LA, Chartoff EH, Gelbart WM. 1995. Genetic characterization and cloning of *Mad*, a gene required for *dpp* function in *Drosophila*. *Genetics* 139:1347–1358.

Shimmi O, Newfeld SJ. 2013. New insights into extracellular and post-translational regulation of TBF-β family signaling pathways. *J Biochem*. 154:11–19.

Siegmund T, Lehmann M. 2002. The *Drosophila* Pipsqueak protein defines a new family of helix-turn-helix DNA-binding proteins. *Dev Genes Evol*. 212:152–157.

Soltani-Bejnood M, Thomas SE, Villeneuve L, Schwartz K, Hong C, McKee BD. 2007. Role of the *mod(mdg4)* common region in homolog segregation in *Drosophila* male meiosis. *Genetics*. 176:161–180.

St. Johnston RD, Hoffmann FM, Blackman RK, Segal D, Grimaila R, Padgett RW, Irick HA, Gelbart WM. 1990. Molecular organization of the *dpp* gene in *Drosophila*. *Genes Dev*. 4:1114–1127.

Stinchfield MJ, Takaesu NT, Quijano JC, Castillo AM, Tiusanen N, Shimmi O, Enzo E, Dupont S, Piccolo S, Newfeld SJ. 2012. Fat facets deubiquitylation of Medea/Smad4 modulates interpretation of a Dpp morphogen gradient. *Development* 139:2721–2729.

Stogios PJ, Downs GS, Jauhal JJ, Nandra SK, Prive GG. 2005. Sequence and structural analysis of BTB domain proteins. *Genome Biol*. 6:R82.

Török T, Tick G, Alvarado M, Kiss I. 1993. P-lacW mutagenesis on the second chromosome of *Drosophila*: isolation of lethals with different overgrowth phenotypes. *Genetics* 135:71–80.

Tsurumi A, Xia F, Li J, Larson K, LaFrance R, Li WX. 2011. STAT is an essential activator of the zygotic genome in early *Drosophila* embryo. *PLoS Genet*. 7:e1002086.

Umulis DM, Shimmi O, O'Connor MB, Othmer HG. 2010. Organism-scale modeling of early *Drosophila* patterning via BMP. *Dev Cell*. 18:260–274.

Wang YC, Ferguson EL. 2005. Spatial bistability of Dpp-receptor interactions during Drosophila dorsal-ventral patterning. *Nature* 434:229–234.

Weber U, Siegel V, Mlodzik M. 1995. *pipsqueak* encodes a novel nuclear protein required downstream of *seven-up* for the development of photoreceptors R3/R4. *EMBO J*. 14:6247–6257.

Weiss A, Charbonnier E, Ellertsdóttir E, Tsirigos A, Wolf C, Schuh R, Pyrowolakis G, Affolter M. 2010. A conserved activation element in BMP signaling during *Drosophila* development. *Nat Struct Mol Biol*. 17:69–76.

Wisotzkey RG, Johnson AN, Takaesu NT, Newfeld SJ. 2003. α/β hydrolase2, a predicated gene adjacent to *Mad* in *Drosophila*, belongs to a new global multigene family and is associated with obesity. *J Mol Evol*. 56:351–361.

Wisotzkey RG, Quijano JC, Stinchfield MJ, Newfeld SJ. 2014. New gene evolution in the Bonus-TIF1-γ/TRIM33 family impacted the architecture of the vertebrate dorsal-ventral patterning network. *Mol Biol Evol*. 31:2309–2321.

Whelan S, Goldman N. 2001. A general empirical model of protein evolution from multiple protein families using a maximum-likelihood approach. *Mol Biol Evol*. 18:691–699.

Xie T, Spradling AC. 1998. *dpp* is essential for the maintenance and division of germline stem cells in the *Drosophila* ovary. *Cell* 94:251–260.

Xiong WC, Montell C. 1993. *tramtrack* is a transcriptional repressor required for cell fate determination in the *Drosophila eye*. *Genes Dev*. 7:1085–1096.

Xu L, Yao X, Chen X, Ju P, Zhang B, Ip YT. 2007. Msk is required for nuclear import of TGF-β/BMP-activated Smads. *J Cell Biol*. 178:981–994.

Zeng Z, de Gorter D, Kowalski M, ten Dijke P, Shimmi O. 2014. Ter94/VCP is a novel component in BMP signaling. *PLoS One* 9:e114475.